Available online at www.sciencedirect.com

ScienceDirect

Energy Procedia 74 (2015) 4 – 14

Energy Procedia

International Conference on Technologies and Materials for Renewable Energy, Environment and Sustainability, TMREES15

Synthesis of Carbon Nanofibers from Decomposition of Liquid Organic Waste from Chemical and Petrochemical Industries

Ali Sami[a], Muthana Mohammed[b*], Ahmad Dhary[b]

[a] College of Education for Pure Sciences , University of Al Anbar, Iraq
[b] School of Chemistry, College of Physical and Applied Sciences, Bangor University, UK

Abstract

This work investigates the possibility of using electrocracking for the decomposition of liquid organic waste from chemical and petrochemical industries. This approach yields a gas containing 22-23% acetylene and a wide range of valuable products from lower olefins, paraffin, and hydrogen. The acetylene concentration reported herein is unattainable by other processes for the production of acetylene from hydrocarbon feedstock, and this method is more environmentally friendly than the carbide method. Electrocracking gas is a very promising raw material for the synthesis of carbon nanostructures and carbon nanofibers (CNFs) in particular, and its use for these purposes creates viable preconditions for the establishment of an integrated technology for the utilization of liquid organic waste. The electric discharge process has a marked advantage in that the electric power consumption is low (8-10 kW.hr per 1 m^3 of C_2H_2). The growth of carbon nanofibers from the Ni-Al_2O_3-catalysed decomposition of electrocracking gas at temperatures of 250–550 °C and electrocracking gas space velocities of 1500-3000 h^{-1} has been investigated in a fixed bed reactor. Scanning electron microscopy (SEM), X-ray powder diffraction (XRPD), and Raman spectroscopy were used to characterize the nanofibers. We demonstrate that carbon nanofibers with diameters mostly between 21.3 and 60.6 nm can be synthesized uniformly and densely on the catalyst.

Peer-review under responsibility of the Euro-Mediterranean Institute for Sustainable Development (EUMISD)

Keywords: decomposition; electrocracking gas; liquid organic waste; carbon nanofibers; fixed bed reactor

* Corresponding author. Tel.: ; +44-744-2751-714 ; +964-78-0313-4081.
E-mail address: hello201077@yahoo.com

Peer-review under responsibility of the Euro-Mediterranean Institute for Sustainable Development (EUMISD)
doi:10.1016/j.egypro.2015.07.511

1. Introduction

The increasing demand for unsaturated hydrocarbons as raw materials in the petrochemical industry has encouraged the development of new processes aimed at utilizing new raw materials, increasing yields, and minimizing energy requirements. One such topic of investigation is the cracking of high-molecular-weight hydrocarbons at high temperatures and over very short times using electrocracking techniques and energy beams [1-3]. The process of electrocracking is based on excitation (by certain methods) of an electric arc discharge between electrodes placed inside a liquid feedstock. The plasma formed as a result of the electric discharge, with a temperature in the range of 5000 to 10000 K, interacts with the feedstock and induces its thermal decomposition, yielding gases composed of hydrogen, acetylene, methane, ethylene, and fine carbon black [4]. The first reactor used for the decomposition of liquid hydrocarbons by electric arc discharge featured two graphite electrodes and was constructed in the 19th century by Pechuro and Pesin, and the first patent for such a reactor was granted in the 1970s [3].

The electrocracking process has been the subject of intense research because the acetylene concentration resulting from the decomposition of liquid hydrocarbon feedstock can be as high as 30% vol. Acetylene is in high demand as a basic monomer for the synthesis of a variety of chemicals. In recent years, there has been an increase in demand for C_3-C_4 olefins. One way to obtain C_3-C_4 olefins is using ethylene dimerization (oligomerization) [5,6].

A mixture of high-molecular-weight compounds and soot can be used to produce highly effective sorbents. The heat treatment and sequential activation of an oxidative mixture yields a carbon-carbon material with an adsorption surface of ~ 680 m^2/g. The high acetylene content in electrocracking gas can be used in the pyro-densification of carbon materials to obtain carbon-carbon composites, similar sibunit. The pyro-densification of carbon nanofibers (CNFs) allows materials to be obtained with a much greater sorption capacity than their corresponding sibunits; thus, CNFs are currently the object of significant interest for use as a catalyst support [7,8]. It is now recognized that when carbon materials are used as a catalyst support or catalyst, their surface area, porosity, structure, and surface chemistry affect not only the catalyst preparation process with respect to the active metal dispersion on the CNFs but also the activity and selectivity of the resulting CNF-supported catalysts [9-11].

Carbon nanofibers and nanotubes are generally grown by conventional thermal chemical vapour deposition (CVD), and electric arc discharge is one of the most important methods developed to produce CNTs and CNFs. Various carbon-containing gases, such as CH_4, C_2H_4, C_2H_2, and CO, are used as the carbon source, and Fe, Ni, Co, and Cu are utilized as catalysts for the decomposition of carbon-containing gases [12-15,7]. Studies by [7] showed that the decomposition of electrocracking gas over γ-Fe_2O_3 formed CNFs (prepared by the decomposition of a diesel fraction) with different morphologies and graphitization degrees. This method has the advantages of a high yield, high selectivity and low cost relative to traditional physical methods, such as laser ablation and chemical vapour deposition. It was demonstrated that the use of electrocracking gas is promising for the synthesis of carbon nanofibers. This approach allows one to utilize organic liquid waste from chemical industries and obtain a valuable carbon material and hydrogen at moderate temperatures.

Nickel catalysts prepared by co-precipitation have been widely used in the hydrogenation and dehydrogenation reactions of hydrocarbons. In these processes, carbon formation on the catalysts has been generally considered harmful, as it causes catalyst deactivation [16]. However, in recent years, such carbon, often with a filamentous or fibrous texture, has become the purpose of production due to its special physical and chemical properties [17]. A nickel-alumina composite catalyst derived from the activation of coprecipitated Feitknecht compound (FC) has been designed and tested [18]. This catalyst grows carbon fibers from methane at a high rate at 500 ºC [18]. It has been proposed that a strong interaction between nickel and alumina inherited from the FC structure enhanced the activity. Carbon nanofibers generated from the Feitknecht compound (FC) Ni-Al2O3 catalysed the decomposition of methane at 500 ºC and correspondingly increased the CNF growth rate [19]. The activity of the Ni–Al_2O_3 catalysts for methane decomposition to produce hydrogen and carbon nanofibers was investigated. In NiO–Al_2O_3 samples calcined at 300–600 ºC, only NiO phases were identified, while the samples calcined at 750 ºC revealed the formation of segregated $NiAl_2O_4$ spinel [20].

In the current investigation we have extended these experiments to explore the sequence of events that occur when organic liquid wastes are used as raw materials for electrocracking, thus producing a gas that serves as a

carbon source for the synthesis of carbon nanofibers and providing an opportunity to ameliorate the negative environmental impact of organic waste disposal.

2. Experimental

2.1. Production of electrocracking gas

The liquid organic waste used in this investigation was obtained from a local refinery, and its physico-chemical characteristics are given in Table 1.

Table 1. Physico-chemical characteristics of liquid organic waste.

Tests	Liquid organic waste
Specific gravity at 15.5 °C	0.897
API gravity	22.41
Viscosity at 40 °C (mm^2s^{-1})	4.539
Distillate at 300 °C (vol%)	66.4
Flash point (°C)	113
Sulphur content (wt%)	1.090

The equipment used in this investigation included a laboratory reactor for the decomposition of liquid organic waste in low-voltage electrical discharges, as shown schematically in Figure 1.

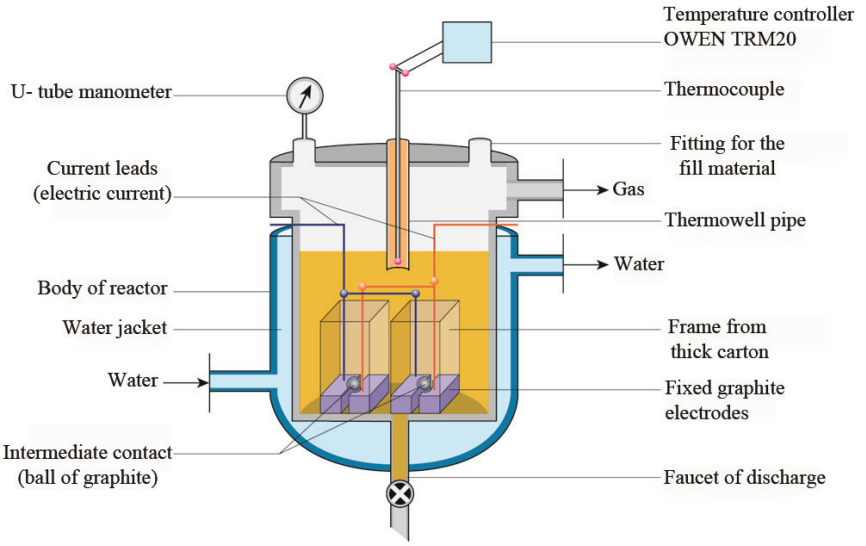

Figure 1. Schematic of the reactor used in the decomposition of liquid organic waste.

The reactor is a stainless-steel vertical cylinder with a water jacket designed for the loading of 700 ml of raw material. This container holds fixed stationary graphite electrodes in the form of graphite rods arranged in parallel with a spacing of 1 mm. On the electrodes, there is a mobile intermediate contact, and a graphite ball with a diameter of ~6.5 mm is positioned between the rods. When voltage from the power supply is applied to the

stationary electrodes and a ball arc discharge occurs, raw materials decompose, producing gas and soot. The gas was collected to study the result of decomposing the electrocracking liquid organic waste fractions. The gas composition is given in Table 2.

Table 2. Composition of the electrocracking gas liquid organic waste.

component	% vol.
H_2	64 ± 1.0
CH_4	6.4 ± 1.0
C_2H_6	0.7 ± 0.1
C_2H_4	6 ± 1.0
C_3H_6	0.8 ± 0.1
C_2H_2	22.1 ± 1.0

The reactor is filled with a certain amount of the raw materials, after which the installation is sealed. Next, voltage is applied from the power source. The resulting gaseous decomposition products accumulated over the reaction period were analysed by gas chromatography every 20 min.

2.2 Synthesis of carbon nanofibers (CNFs)

As shown in Figure 2, a flowing laboratory setup was used for the synthesis of the CNFs consisted with an integrated reactor. The electrocracking gas was displaced from the electrocracking gas storage by water through a valve, regulated by a control valve, and operated at atmospheric pressure, as set by a water U-tube manometer. The gas flow to the reactor was precisely regulated by calculating the gas hourly space velocity (GHSV) and then sent into a rheometer to ensure that each sample was subjected to the selected GHSV.

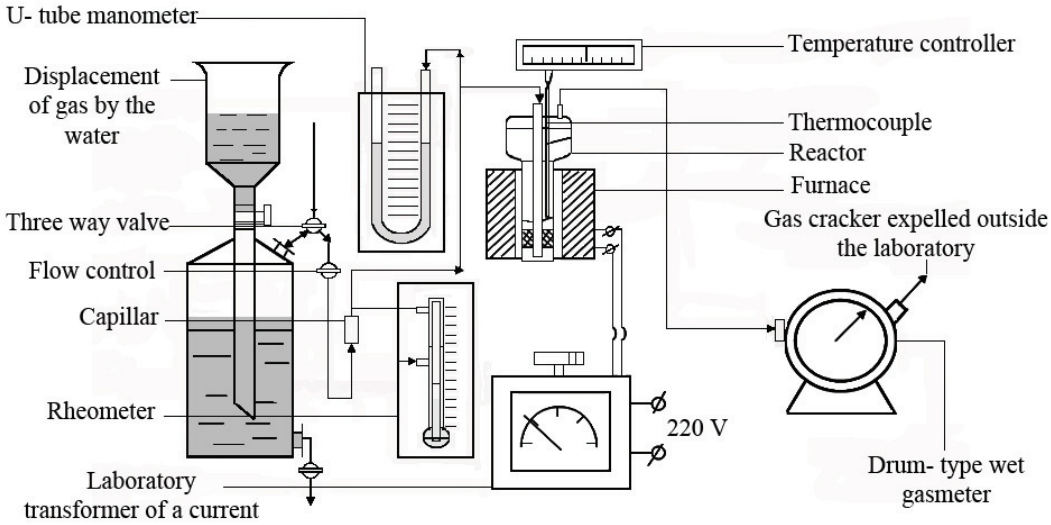

Figure 2. Schematic of the laboratory setup for the synthesis of carbon nanofibers (CNFs).

The gas flow was in the direction of the quartz reactor. Catalyst samples (0.2 g) were placed in a fixed bed in the center of the reactor tube (inner diameter, 10 mm) inside a split furnace. The temperature in the reaction zone was measured by a thermocouple and registered. The reaction was followed as a function of time by sampling both the

input and output gas streams at regular intervals and analysing the reactants and products with a LHM-8 gas chromatograph and a thermal conductivity detector (TCD). The current bridge detector was set at -90 mA., and the carrier gas flow (nitrogen) was set at 25 ml/min. The column was 7 m in length and thermostatted at 80 ºC. This chromatograph was specially configured (columns and microvalve switching) for the analysis of light gases, i.e., alkanes (C_1-C_5), alkenes (C_2H_4, C_3H_6), and alkynes (C_2H_2). These experiments were performed using quartz as a reference material under analogous conditions and with the same weight as used in the catalyst experiments to evaluate the reaction selectivity toward carbon nanofiber formation. The total amount of carbon deposited during exposure to the stream was determined by material balance.

2.3 Catalyst preparation

The composite catalyst used in this investigation was obtained from the activation of co-precipitated Feitknecht compound (FC). FC was synthesized by mixing solutions of $Ni(NO_3)_2 \cdot 6H_2O$ and $Al(NO_3)_3 \cdot 6H_2O$ such that the final solution was 3 wt% Ni and 1 wt% Al_2O_3 (Aldrich). The salts were dissolved in distilled water along with a certain molarity of Na_2CO_3 to induce precipitation under vigorous stirring. In this study, we synthesized FC with an atomic ratio of Ni^{2+}/Al^{3+}=3/1(w/w). The precipitate was then washed with D.I. water to remove Na^+ residue. The solution was filtered, and the precipitate dried overnight at 120 °C. Calcination was performed at 500 ºC for 5 h. The calcined catalyst was crushed to a particle size of 300-400 mesh for the catalysed growth. The reduction of the composite catalyst was then carried out at 500 ºC with a mixture of H_2 and N_2 for 1 h. The gases used in this study (hydrogen and nitrogen) were used without further purification.

2.4 Characterization

The nature and characteristics of the carbon nanofibers product were ascertained using a combination of techniques. Scanning electron microscopy (SEM) was performed using a Nova nanoSEM field emission scanning electron microscope (FESEM, FEI Company, Hillsboro, OR) operated under high-vacuum conditions using a Everhart-Thornley (ET) detector as a secondary electron detector and a high-resolution in-lens thermoluminescence detector (TLD). The parameters were 5 kV, a spot size 2.7, 3.5-4 mm a working distance, a 30-μm objective aperture, and magnifications of 25-200K. X-ray powder diffraction (XRPD) pattern was obtained using a Rigaku Smart-Lab diffractometer in reflection (Bragg-Brentano) geometry using a line source X-ray beam. The X-ray source is a Cu long fine focus tube operated at 40 kV and 44 mA. The diffractometer was operated to give peak widths of $2\theta \leq 0.1°$ using a continuous scan of 2θ=6°/min with an effective step size of 2θ=0.02°.

Raman spectra were obtained using a Renishaw inVia Raman microscope. The inVia system interfaces a Leica DMLM microscope to a Raman spectrometer. Each sample was placed on a motorized x-, y-stage underneath a 50x objective and excited by a polarized diode laser (785 nm) through the microscope. The system was calibrated using the 520.5 cm^{-1} peak of an internal silicon wafer.

3. Results and discussion

3.1 Flow reactor studies

In an initial series of experiments, various electrocracking gas mixtures were passed over the Ni-Al_2O_3 catalyst, and the amount of solid carbon produced was determined as a function of reaction temperature under survey conditions including temperature, feed composition, and gas hourly space velocity (GHSV). The deactivation rates depended strongly on temperature and composition. Under standard conditions (electrocracking gas: 64% H_2, 6.4% CH_4, 0.7% C_2H_6, 6%C_2H_4, 0.8% C_3H_6, 22.1% C_2H_2; 200 mg of catalyst used with a 3:1 atomic ratio of Ni^{2+}/Al^{3+}; 6.66, 9.60, and 13.00 cm^3/min total flow; GHSV of ~1500, 2200, and 3000 h^{-1}, respectively), it is evident that the optimum conditions for this reaction are realized at approximately 250-550 ºC. As the temperature is shifted either above or below this level, there is a precipitous drop in the yield of solid carbon. The data presented in Table 3 show

that the optimum yields of solid carbon occur at 350 ºC and a gas hourly space velocity of 3000 h^{-1}. An example of the typical dependence is shown in Figure 3.

Under these conditions, the yield of carbon nanofibers was ~44% on a theoretical basis. Subsequent analysis demonstrated that catalytic decomposition of C_2H_2 was the major route for the growth of carbon nanofibers. It can be seen that at low temperatures (to ~350 °C), carbon was formed because of the decomposition of acetylene. Above ~350 °C, an increase in the concentrations of methane and ethane in the gas suggested that acetylene hydrogenation occurred along with decomposition. As the temperature increased further, other hydrocarbons from the electrocracking gas were involved in the carbon formation reactions, and only H_2 and CH_4 were present in the effluent gases at 550 °C. In this set of experiments, we have endeavoured to probe the effect of temperature on the overall solid carbon yield. We found an amorphous carbon content of 10% in the yield of CNFs at high temperatures, especially 550 ºC. It is also evident that catalytic activity is constant at temperatures up to 550 ºC. When the reaction was performed above 550 ºC, a sudden drop in activity was observed approximately 40 min into the reaction. According to a mechanism proposed in the literature [12], the nature of the carbon-containing gas as well as the catalyst composition plays an important role in the formation of the microstructure and morphology of CNFs.

Table 3. Percentage gas phase product distribution as a function of synthesis conditions over Ni-Al_2O_3 (3:1) for 40 min.

Synthesis conditions		Effluent gas composition, vol.%						Carbon yield, g/(l gas)
Temperature, °C	GHSV h^{-1}	H_2	CH_4	C_2H_6	C_2H_4	C_3H_6	C_2H_2	
	1500	69.5	12.3	0.7	8	1.7	7.8	0.06
250	2200	72.41	12.8	0.8	8.1	1.75	4.14	0.08
	3000	72.6	13	0.84	8.49	1.95	3.12	0.10
	1500	75.03	13.45	0.98	8.76	1.78	0	0.12
350	2200	75.2	12.95	0.97	9.13	1.75	0	0.14
	3000	76.41	12.83	1.21	8	1.55	0	0.16
	1500	78.77	14.33	1.1	4.7	1.1	0	0.10
450	2200	82.29	11.74	1.14	4.5	0.33	0	0.12
	3000	84.43	10.5	0.74	4.23	0.1	0	0.14
	1500	89	9.6	0.3	1.1	0	0	0.08
550	2200	90.15	8.83	0.28	0.74	0	0	0.10
	3000	92.43	7.57	0	0	0	0	0.12

Generally speaking, the affinity of different metals with different carbon-containing gases controls the degree of dissolved carbon supersaturation in metal and consequently the microstructure of the carbon filament deposited on the metal.

Thus, it is not surprising that we also observed the formation of pyrolytic carbon along with carbon nanofibers in the thermocatalytic decomposition of hydrocarbons. Soot may also be formed. Therefore, studies using quartz as inert packing were performed under analogous conditions to evaluate the reaction selectivity of carbon nanofiber formation.

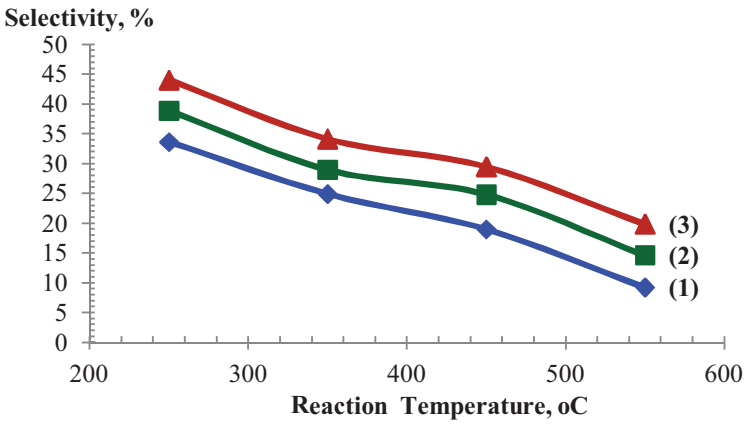

Figure 3. Selectivity of CNF formation from the Ni-Al_2O_3 (3:1) catalysed decomposition of electrocracking gas at GHSV values of (1) 1500, (2) 2200, and (3) 3000 h^{-1} as a function of reaction temperature.

These data were calculated using carbon atom mass balances according to the procedure described in Appendix A.

3.2 Characterization of the solid carbon product

Figure 4 shows a typical XRPD pattern of the CNFs. The high peak at 26.552º can be indexed to the (002) diffraction plane. The diffraction peak of the CNF was clear regardless of the catalyst or carbon-containing gas used

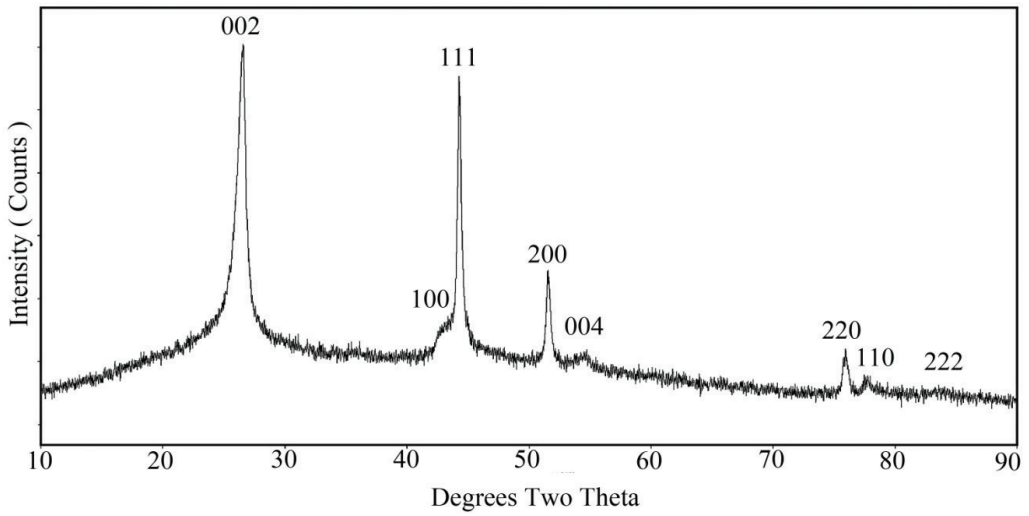

Figure 4. Representative X-ray powder diffraction pattern for the carbon nanofibers produced. The pattern corresponds to nanofibers grown at 250 ºC and a total electrocracking gas flow rate of 6.66 cm^3/min.

for the synthesis, indicating that the CNFs were highly graphitized, close to ideal and highly ordered [21]. The d_{002} spacing of the CNFs varied by 0.335 nm, and the crystallite size (Lc) was estimated by analysing the CNF peak using the Scherrer equation, $Lc=k\lambda/(\beta \cos\theta)$, where k is a constant (the shape factor, approximately 0.9), λ is the X-

ray wavelength (0.15405 nm), and β is the full width at half maximum (FWHM) of the diffraction line, and θ is the diffraction angle. The carbon nanofiber crystal size was 8.64 nm. The other three peaks at 2θ=42.88º, 54.69º, and 77.51º can be indexed to the (100), (004), and (110) diffraction planes of hexagonal graphite (JCPDS card files, no. 41-1487). The Ni peaks are much sharper because large catalyst particles could be easily dispersed in the fibers and gave distinct nickel peaks: 2θ=44.27º, 51.54º, and 75.91º indexed to Ni(111), Ni(200), and Ni(220) diffraction peaks of the cubic phase of nickel (JCPDS card files, no. 04-0850). The weak peak observed at 2θ=84º can be attributed to Ni(222). The catalyst particles undergo surface reconstruction to form geometrical shapes, which were able to promote the formation of carbon nanofibers under certain growth conditions in terms of catalyst, gas, and temperature [22-24]. No impurities were observed in the XRPD pattern.

Rodriguez reported that there is a subtle relationship between the degree of ordering in the deposited CNFs and the ability of the metal catalyst particle to participate in a strong interaction with graphite [25]. He also found that the metal catalyst, which has good wetting characteristics with respect to graphite, forms highly graphitic carbon nanostructures. The Raman spectrum of the CNF sample (Figure 5) obtained from electrocracking gas exposed to Ni-Al_2O_3 catalyst at 250 ºC exhibited the D and G peaks characteristic of CNFs. The peak centered at ~1355 cm^{-1} corresponding to the A_{1g} vibrational mode (the so-called D-mode) are usually assigned to disordered sp^2 carbon material or defect positions in the graphitic sheets of CNFs [26]. The peak at 1578 cm^{-1} (the so-called G-mode) is assigned to well-ordered graphite (normal graphite structure). The D′ peak (1685 cm^{-1}) is the disorder-induced peak and is associated with the maximum vibrational density of states. This peak is a result of the splitting of the E_{2g} degenerate mode in group theoretical analysis; it is located near the G peak (in-plane E_{2g} mode) and looks like a shoulder of the G peak. It is to be noted that the D′ peak can also be found in the Raman spectra of carbon nanofibers, multi-walled carbon nanotubes, graphene, and coke [26].

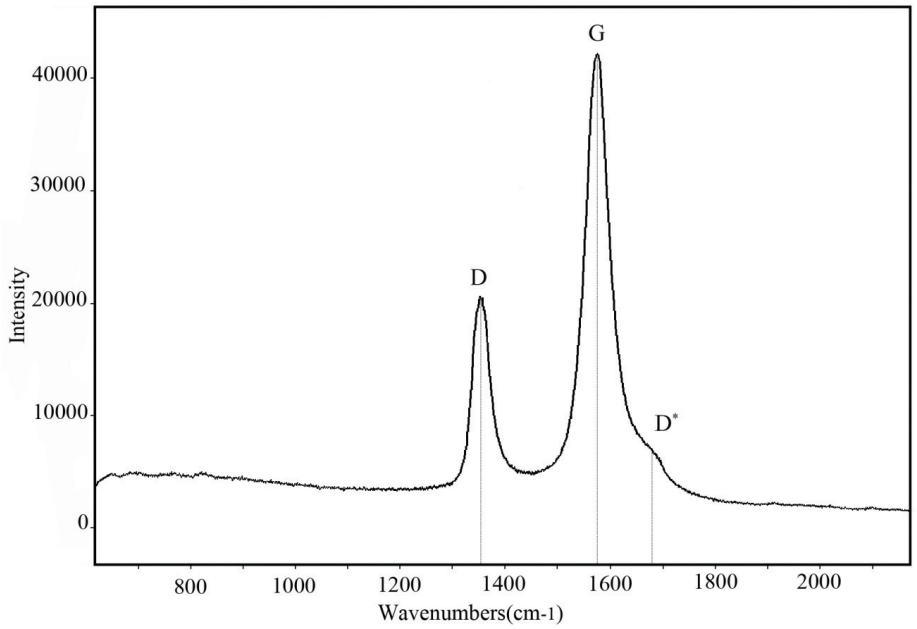

Figure 5. Representative Raman spectra for the carbon nanofibers produced showing the characteristic D and G peaks of CNFs and the disordered D′ peak at 1685 cm^{-1}.

The intensity ratio of the D peak and G peaks, I_D/I_G, has been employed to characterize the graphitization degree of carbon materials [27-29]. According to our experiment, we know that the value of I_D/I_G is approximately 0.79. For crystalline graphitic carbons, the G peak occurs at 1580 cm^{-1}. However, the G peak in Figure 5 occurs at 1578 cm^{-1}. The XRPD spectra of solid carbon obtained from electrocracking gas on the Ni-Al_2O_3 catalyst featured a sharp

peak at 2θ=26.552º (d=3.35º), which corresponds to the (002) graphitic basal plane and is typically observed for graphite.

Under the reaction conditions used in this investigation, FESEM images revealed that the solid carbon product consisted entirely of carbon nanofibers. The materials did, however, exhibit physical and morphological characteristics that were a function of the catalyst and reactant compositions. Figure 6a presents a typical FESEM image of the product of reacting the Ni-Al_2O_3 catalyst in the electrocracking gas mixture, showing thin, well-formed filaments among much wider nanofibers and soot. The specimen does not contain free soot, but the non-uniformity of the amorphous carbon coating on some fibers results in the formation of soot-like nanoballs along the fibers. As previously reported by Masuda et al. [30,31], this is caused by metal particles seeded over preformed nanofilaments. Generally, there are large differences in the fiber diameters and, despite these balls, the fibers are quite straight. Figure 6b shows that the CNFs have diameter ranging from 21.3 nm to 60.6 nm and lengths exceeding several micrometers. Closer observations reveal that most of the CNFs with smooth and round surfaces are bent, and a few are curly. Neither soot nor irregularities are observed along the length of the nanofibers, and the fibers appear quite uniform in size.

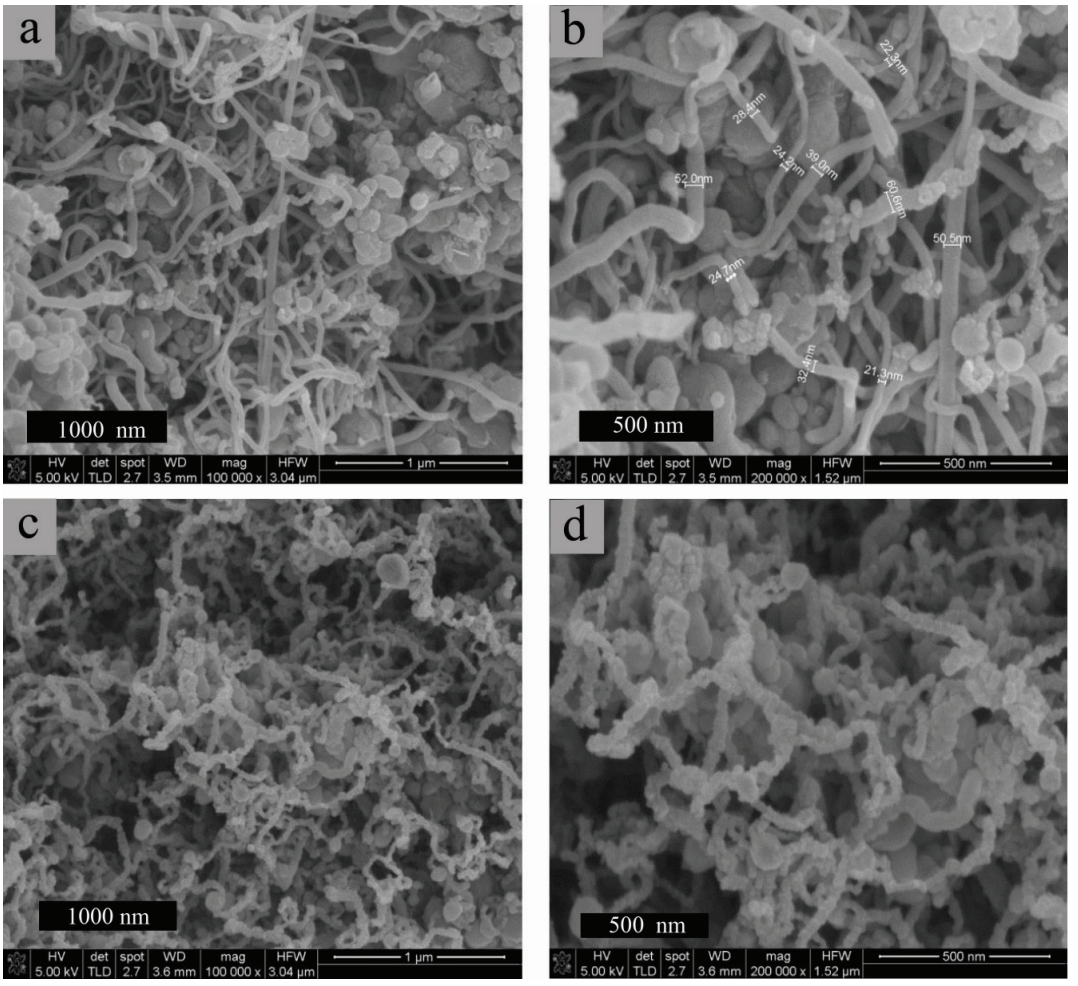

Figure 6. Field emission scanning electron microscope (FESEM) images of the carbon nanofibers synthesized from the Ni-Al_2O_3 (3:1) catalysed decomposition of electrocracking gas (a and b) at 250 ºC. The inset shows the formation of soot-like nanoballs along the fibers associated with the "fishbone" structure (c and d) at 550 ºC.

4. Conclusions

In the current investigation, the possibility of synthesizing carbon nanofibers from electrocracking products of the decomposition of liquid organic waste in a fixed bed reactor was investigated. The highest conversion of the carbon-containing electrocracking gas reactant towards solid carbon occurred at 350ºC and a gas hourly space velocity of 3000 h^{-1} via interaction with a Ni–Al_2O_3 catalyst. Subsequent analysis demonstrated that the catalytic decomposition of C_2H_2 was the major route for the growth of carbon nanofibers. We found an amorphous carbon content of 10% in the CNF yield at high temperatures, especially 550 ºC. The XRPD and Raman analyses indicate that CNFs exhibit d_{002} spacing, and the crystallite size (Lc) featured a sharp peak at d=3.35º, corresponding to the (002) graphitic basal plane and typical of graphite. The platelet morphology of the CNFs synthesized on the Ni-Al_2O_3 catalyst was observed by FESEM, which suggested the carbon layers of nanofibers have a uniform orientation that perpendicular to the fibre axis and that the graphite layers are stacked with a fishbone structure and a hollow core. However, the carbon nanofibers have a crooked morphology.

Acknowledgements

The authors greatly appreciate the valuable help of Mr. Brett D. Bobzien (Triclinic Labs, West Lafayette, Indiana) with the preparation of XRPD, Raman and SEM data.

Appendix A

The relative amounts of solid carbon generated from the decomposition of electrocracking gas (EG) as a function of the reactant gas composition were calculated according to the following procedure. Consider the material balance in the deposition reactions,

$$[H_2]^i m_r^i + [CH_4]^i m_r^i + [C_2H_6]^i m_r^i + [C_2H_4]^i m_r^i + [C_3H_6]^i m_r^i + [C_2H_2]^i m_r^i \rightarrow [H_2]^o m_r^o + [CH_4]^o m_r^o + [C_2H_6]^o m_r^o + [C_2H_4]^o m_r^o + [C_3H_6]^o m_r^o + [C_2H_2]^o m_r^o + mC$$

where $[M]^i$ = concentration of component M in the input gas
$[M]^o$ = concentration of component M in the output gas
m_r^i, m_r^o = mass of gas (= M*n) for the input and output gases, respectively
The solid carbon yield from electrocracking gas (EG) decomposition can be written as

$$\Delta C = \text{mass of carbon(gm) from EG}_{\text{input}} - \text{mass of carbon(gm) from EG}_{\text{output}}$$

$$\text{Yield of CNF} = \frac{\Delta C}{\text{Volume of gas}_{\text{input}}} \ (\text{gm/L})$$

which is

$$\text{Total of CNF} = \text{yield of CNF}_{\text{presence of the catalyst}} - \text{yield of CNF}_{\text{presence of the quartz}}$$

References

[1] Venugopalan M, Scott TW. Rates of formation of hydrogen, methane and ethane in xylene plasmas. Zeitschrift für Phys. Chem. 1977; 108: 157-165.

[2] Taki K. Studies of the electric discharge of organic compounds. I. The decomposition of toluene in 10-MHz and 2450-MHz discharges. Bull. Chem. Sot. Jap. 1970; 43: 1574-1577.

[3] Pechuro NS, Pesin OJ. US Patent 1970; No. 3519551.

[4] Nikolaev AI, Estrin RI, Peshnev BV, Kuz'micheva GM, Tret'yakov VF. Electrocracking of petroleum products: Effect of process duration on characteristics of carbon black. J Solid Fuel Chemistry 2007; 41: 97-99.

[5] Trimma DL, Liub Irene OY, Cantc NW. The oligomerization of acetylene in hydrogen over Ni/SiO_2 catalysts: Product distribution and pathways. J Molecular Catalysis A: Chemical 2008; 288: 63–74.

[6] Rodriguez J C, Marchi A J, Borgna A, Monzon A. Effect of Zn content on catalytic activity and physicochemical properties of Ni-based catalysts for selective hydrogenation of acetylene. J Catal. 1997; 171: 268–278.

[7] Nikolaev A I, Peshnev B V, Ismail A S. Production of carbon nanofibers from the gas electrocracking on iron oxide catalyst. J Solid Fuel Chemistry 2009; 4: 35- 37.

[8] Peshnev BV, Nikolaev A I ,Pilipeiko A Yu, Estrin B V. Structural and Physicochemical Characterization of Carbon Nanofibers by the COMPAS Method. J Solid Fuel Chemistry 2007; 41: 52-57.

[9] Auer E, Freund A, Pietsch J, Takke T. Carbons as supports for industrial precious metal catalysts. Appl. Catal. A: General 1998; 173: 259–271.

[10] Radovic LR, Rodriguez-Reinoso F. In: Thrower PA, editor. Chemistry and Physics of Carbon, Carbon materials in catalysis. New York: Marcel Dekker; 1997. Vol. 25. p. 243–358.

[11] Schlogl R. In: Ertl G, Knzinger H, Weitkamp J, editors. Preparation of solid catalysts. Wiley-VCH: Weinheim; 1999. p. 150–240.

[12] Baker RTK. Catalytic growth of carbon filaments. Carbon. 1989; 27: 315-323.

[13] Ebbesen TW, Ajayan PM. Large-scale synthesis of carbon nanotubes. Nature 1992; 358: 220-222.

[14] Kim MS, Rodriguez NM, Baker RTK. The role of interfacial phenomena in the structure of carbon deposits. J Catal. 1992; 134; 253-268.

[15] Reshetenko TV, Avdeeva LB, Ismagilov ZR, Pushkarev VV, Cherepanov SV, Chuvilin A L, Likholobov VA. Catalytic filamentous carbon: Structural and textural properties. Carbon 2003; 41: 1605-1615.

[16] Trimm DL. The formation and removal of coke from nickel catalyst. Catal. Rev. Sci. Eng. 1977; 16:155-189.

[17] Rodriguez N M, Kim MS, Baker RTK. Carbon nanofibers: a unique catalyst support medium. J. Phys. Chem. 1994; 98: 13108-13111.

[18] Li YD, Chen JL, Chang L. Catalytic growth of carbon fibers from methane on a nickel-alumina composite catalyst prepared from Feitknecht compound precursor. Appl. Catal. A 1997; 163: 45-57.

[19] Li YD, Chen JL, Chang L, Zhao J. Feitknecht compound used as the precursor of the catalyst for the catalytic growth of carbon fibers from methane. Studies in Surface Science and Catalysis 1998;118: 321-329.

[20] Chen JL, Ma Q, Rufford TE, Li YD, Zhu Z. Influence of calcination temperatures of Feitknecht compound precursor on the structure of Ni–Al 2O 3 catalyst and the corresponding catalytic activity in methane decomposition to hydrogen and carbon nanofibers. Appl. Catal. A-GEN 1997; 362: 1-7.

[21] Okpalugo TIT, Papakonstantinou P, Murphy H, Mclaughlin J, Brown NMD. Oxidative functionalization of carbon nanotubes in atmospheric pressure filamentary dielectric barrier discharge (APDBD).Carbon 2005; 43: 2951.

[22] Rodriguez NM, Chmbers A, Baker RTK. Catalytic engineering of carbon nanostructures. Langmuir 1995; 11: 3862–3866.

[23] Krishnankutty N., Rodriguez NM, Baker RTK. Effect of copper on the decomposition of ethylene over an iron catalyst. J. Catal. 1996;158: 217–227.

[24] Chambers A, Baker RTK. Influence of chlorine on the decomposition of ethylene over iron and cobalt particles. J Phys. Chem. B 1997; 101: 1621–1630.

[25] Rodriguez NM. A review of catalytically grown carbon nanofibers. J Mater Res 1993;8:3233–49.

[26] Tai FC, Wei C, Chang SH, Chend WS. Raman and x-ray diffraction analysis on unburned carbon powder refined from fly ash. J Raman Spectrosc 2010; 41: 933–937.

[27] Singh C, Quested T, Boothroyd CB, Thomas P, Kinloch IA, Abou-Kandil AI, Windle A H. Synthesis and characterization of carbon nanofibers produced by the floating catalyst method. J Phys. Chem. B 2002; 106: 10915-10922.

[28] Liu Y, Pan C, Wang J. Raman spectra of carbon nanotubes and nanofibers prepared by ethanol flames. J. Mater. Sci. 2004; 39: 1091-1094.

[29] *Liao KH*, *Ting JM.* Effects of Ni-catalyst characteristics on the growth of carbon nanowires. Carbon 2004; 42: 509-514.

[30] 34Masuda T, Mukai SR, Hashimoto K. The liquid pulse injection technique: a new method to obtain long vapor grown carbon fibers at high growth rates, Carbon 1993;31(5):783–787.

[31] Martin-Gullon I, Vera J, Conesa JA, Gonz´lez JL, Merino C. Differences between carbon nanofibers produced using Fe and Ni catalysts in a floating catalyst reactor. Carbon 2006; 44: 1572–1580.